

Catalysis Science & Technology

Accepted Manuscript



This article can be cited before page numbers have been issued, to do this please use: Z. Gao, Y. Hong, Z. Hu and B. Xu, *Catal. Sci. Technol.*, 2017, DOI: 10.1039/C7CY01569K.



This is an Accepted Manuscript, which has been through the Royal Society of Chemistry peer review process and has been accepted for publication.

Accepted Manuscripts are published online shortly after acceptance, before technical editing, formatting and proof reading. Using this free service, authors can make their results available to the community, in citable form, before we publish the edited article. We will replace this Accepted Manuscript with the edited and formatted Advance Article as soon as it is available.

You can find more information about Accepted Manuscripts in the [author guidelines](#).

Please note that technical editing may introduce minor changes to the text and/or graphics, which may alter content. The journal's standard [Terms & Conditions](#) and the ethical guidelines, outlined in our [author and reviewer resource centre](#), still apply. In no event shall the Royal Society of Chemistry be held responsible for any errors or omissions in this Accepted Manuscript or any consequences arising from the use of any information it contains.

Revised manuscript submission: *CY-ART-08-2017-001569*

Transfer Hydrogenation of Cinnamaldehyde with 2-Propanol on Al₂O₃ and SiO₂-Al₂O₃ Catalysts: Role of Lewis and Brønsted Acidic Sites

Zhan-Kun Gao, Yong-Chun Hong, Zhun Hu, Bo-Qing Xu*

Innovative Catalysis Program, Key Lab of Organic Optoelectronics & Molecular Engineering,
Department of Chemistry, Tsinghua University, Beijing 100084, China

* Corresponding author. E-mail address: bqxu@mail.tsinghua.edu.cn

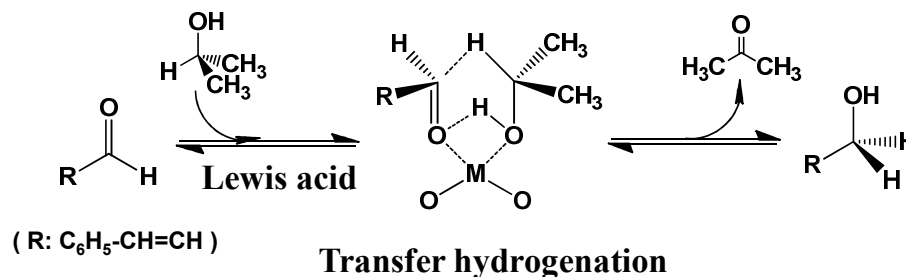
Abstract: Transfer hydrogenation of α,β -unsaturated aldehyde is an important reaction (MPV reaction) for the synthesis of allyl alcohol because of its high selectivity for the hydrogenation at the carbonyl group. The reaction can proceed over many oxide catalysts but the role of acidic and basic sites on the oxide catalyst surface has remained an issue of debate. We report herein the catalytic data of serial Al₂O₃ and SiO₂-Al₂O₃ catalysts for the MPV of cinnamaldehyde at 150 °C using 2-propanol as the H-donor. The surface acidity of the catalysts is adjusted by changing of the calcination temperature between 400 and 1000 °C, and quantified to correlate with the catalyst performance. Surface Lewis acidic sites that are poisoned by pyridine but not by hindered pyridine (lutidine) under the catalyst working conditions are identified as the catalytic sites for the MPV reaction. The lutidine-sensitive surface Brønsted acidic sites, which are among the spectator sites during the MPV reaction, are shown to serve as the catalytic sites for the cascade cross-etherification reaction between cinnamyl alcohol and 2-propanol. The MPV reaction is also conducted under higher pressure CO₂, the results of which exclude a possible involvement of surface basic sites during the reaction.

Keywords: Solid acids, Acid-base catalysis, Transfer hydrogenation, Selective poisoning, α,β -unsaturated aldehyde, Active sites

Introduction

The selective reduction of unsaturated carbonyl compounds to their corresponding unsaturated alcohols is an important reaction in fine chemical synthesis.¹⁻⁴ Compared to traditional methods of carbonyl reduction by molecular hydrogen (H₂) employing precious metal (such as Au, Pt and Pd) catalyst,⁵⁻⁷ carbonyl reduction via transfer-hydrogenation using alcohols as H-donor under the presence of acid-base oxide catalyst, that is Meerwein-Ponndorf-Verley (MPV) reaction,⁸ would be more promising because of its distinctly high selectivity for producing unsaturated alcohols,⁹ better economic feasibility in terms of catalyst cost,¹⁰ and environmental friendliness.¹¹

MPV reaction between aldehyde (H-acceptor) and alcohol (H-donor) was known earlier to be catalyzed by homogenous Lewis acids (such as aluminum alkoxides) via a six-member ring structured transition state, as shown in Scheme 1.⁸ Heterogeneous acid-base catalysts, including acidic (zeolites, Al₂O₃, etc.),¹²⁻¹⁴ basic (MgO, etc.)¹⁵⁻²⁶ and acid-base bifunctional ones (ZrO₂, etc.),²⁷⁻³¹ were also reported to be efficient for the reaction. However, the nature of the catalytically active sites on these solid oxide catalysts has long remained an issue of much debate.³²⁻³⁷



Scheme 1. Homogeneous Lewis acid catalyzed transfer hydrogenation of cinnamaldehyde with 2-propanol.⁸

As an analog to homogenous catalyst, heterogeneous Lewis acids are also found active for MPV reaction, probably proceeding via a surface transition state with a structure similar to the six-membered ring in Scheme 1. In their study of a series of Zr-containing catalysts, including bulk ZrO₂, supported ZrO₂ (ZrO₂/SiO₂, ZrO₂/TiO₂, ZrO₂/CeO₂), and zirconosilicates (Zr-BEA and Zr-MCM-41), for the MPV reaction between crotonaldehyde and ethanol in the temperature range of 473–573 K, Ivanova et al.¹² showed that the catalyst activity positively correlates to the number of tetrahedral Zr⁴⁺ (Lewis acid) sites in the catalyst samples. Similar

correlation was also reported by Urbano et al.³⁵, who worked on liquid- as well as gas-phase reactions between crotonaldehyde and 2-propanol on ZrO₂ catalysts modified with Al₂O₃, Ga₂O₃ and In₂O₃. In the kinetic study of the reaction between methyl levulinate and 2-butanol on Lewis acidic Zr-BEA zeolites, Leshkov et al.¹³ revealed that H-transfer to the carbon atom in the carbonyl group from the C-H (β -H) of the secondary alcohol could be the rate-limiting step.

Basic solids, like MgO, were also found active for MPV reactions.¹⁵⁻²⁶ Shen et al.¹⁸ reported that the activity of MgO for the MPV reaction between benzaldehyde and ethanol increased with increasing the basic site density according to CO₂-TPD. Similar observations were reported for other MPV reactions on high surface area MgO,¹⁹ CaO-Al₂O₃ mixed oxides²² and La₂O₃/Al₂O₃ catalysts.²³ The contribution of surface basic sites (O²⁻ anions), however, would be complicated by the possible contribution of their conjugated Lewis acidic sites (surface cations such as Mg²⁺ and Ca²⁺).²⁷⁻³¹ The basic sites were proposed to assist the formation of six-membered ring transition state (Scheme 1) at their conjugated Lewis acid sites during the reaction between cyclohexanone and 2-propanol over ZrO₂,²⁷ which seems to be supported by the observation that mixed oxide SnO₂-MgO-Al₂O₃ was more efficient than MgO and MgO-Al₂O₃ in catalyzing the MPV reactions of benzaldehyde and cyclohexanone with 2-propanol.²⁹

Surface Brønsted acidic sites, usually in the form of surface hydroxyl groups, were also regarded as the possible active sites for MPV reactions.^{32,33} On ZrO₂ doped with boron and alkaline earth metal cations, for instance, Brønsted acidic sites of medium to strong acidity, as determined by Raman spectra of adsorbed pyridine, were considered to be active for the reaction between cinnamaldehyde and 2-propanol.³³ However, transformation of surface hydroxyl (Mⁿ⁺-OH) based Brønsted acidic sites to Lewis acidic sites (Mⁿ⁺) by 'ligand-exchange', e.g., with alkoxy group,³⁴ could also occur during reaction, making it difficult to identify the function of Brønsted acidic sites under the reaction conditions. In addition, the presence of Brønsted sites at the catalyst surface would lead to possible cascade etherification reaction during MPV reaction, as the intermolecular dehydration between the alcohol products was considered to happen easily over the Brønsted sites.³⁸⁻⁴⁰ However, little effort has been made to date to quantitatively correlate the surface Brønsted acidity with the

reactivity and product selectivity of the carbonyl reduction during MPV reactions.

Reported herein are the catalytic data of serial Al_2O_3 (Lewis acidic) and $\text{SiO}_2\text{-Al}_2\text{O}_3$ (both Brønsted and Lewis acidic) catalysts for the reduction of cinnamaldehyde (CAL) to cinnamyl alcohol (COL) at 150 °C by transfer hydrogenation using 2-propanol (2POL) as the H-donor. The surface acidity of the catalysts was fine-tuned by systematical change of their calcination temperature between 400 and 1000 °C and quantified to correlate with the catalyst performance. We show that surface Lewis acidic sites are solely responsible for the transfer hydrogenation catalysis. Surface Brønsted acidic sites are confirmed to be responsible for catalyzing the cascade cross-etherification reaction, leading to formation of 1-cinnamyl 2-propyl ether (CPE) from COL.

1. Experimental

1.1 Sample preparation

The Al_2O_3 samples were prepared by calcination of an $\text{Al}(\text{OH})_3$ hydrogel at different temperatures T ($T = 450\text{--}1000$ °C) in flowing air ($50\text{ mL}\cdot\text{min}^{-1}$, STP) for 5 h, as previously reported.⁴¹ The hydrogel was obtained by hydrolysis of $\text{Al}(\text{NO}_3)_3\cdot 9\text{H}_2\text{O}$ (AR, Dongfang Chemical Reagent Company, Beijing) with an aqueous solution of ammonia with the final pH controlled at $\text{pH} = 10$. The calcined samples were denoted as $A\text{-}T$ according to the calcination temperature T . $\text{SiO}_2\text{-Al}_2\text{O}_3$ was obtained from Sasol (SIRAL30, $\text{SiO}_2\text{:Al}_2\text{O}_3 = 30\text{:}70$ wt/wt), which was calcined at $400\text{--}800$ °C in flowing air ($50\text{ mL}\cdot\text{min}^{-1}$, STP) for 5 h prior to use. The calcined $\text{SiO}_2\text{-Al}_2\text{O}_3$ samples were denoted as $\text{SA}\text{-}T$ ($T = 400\text{--}800$ °C).

1.2 Characterizations

Surface areas of the samples were determined using N_2 adsorption–desorption isotherms measured at -196 °C on a Micromeritics ASAP 2010C instrument using BET model. Prior to the measurements, the samples were degassed under vacuum at 200 °C for 5 h. X-ray diffraction (XRD) patterns were recorded on a Bruker D8 Advance X-ray diffractometer with a Ni-filtered $\text{Cu K}\alpha$ ($\lambda = 0.15406$ nm) radiation at 40 kV and 40 mA. Data analysis was performed using JADE (Materials Data, Inc., Livermore, CA).

The surface acidity of $A\text{-}T$ was measured by temperature programmed desorption of NH_3 ($\text{NH}_3\text{-TPD}$)⁴¹⁻⁴⁶ and FTIR spectroscopy of adsorbed pyridine.⁴¹⁻⁴³ The $\text{NH}_3\text{-TPD}$ measurement

was conducted on a catalyst analyzer (BEL-A, Japan) equipped with a mass spectrometer (Inprocess Instruments, GAM200) as the detector. The sample (ca. 50 mg) was loaded in a quartz reactor (I.D.= 4 mm) and pretreated in a synthetic air (20 vol% O₂ in Ar) flow (50 mL·min⁻¹, STP) at the sample calcination temperature (*T*) for 0.5 h, and then cooled to 100 °C in flowing dry Ar (50 mL·min⁻¹, STP) for adsorption of NH₃, which was conducted by switching the reactor to a flow of 1.9 vol% NH₃ in Ar for 0.5 h. The reactor was then purged with flowing dry Ar (40 mL·min⁻¹) until a stabilized baseline was obtained. NH₃-TPD profiles was measured by recording the signal of *m/z* = 15 with a temperature ramp of 10 °C·min⁻¹ up to 800 °C. FTIR measurement of adsorbed pyridine was performed on a Perkin-Elmer FTIR System 2000 spectrophotometer in the transmission mode with a quartz-lined stainless steel *in situ* IR cell with optical path length less than 5 mm.⁴¹⁻⁴³ Self-supporting sample wafers (10 mg·cm⁻²) were pretreated in flowing 20 vol% O₂/Ar (40 mL·min⁻¹) at 400 °C for 2 h and cooled to 100 °C in flowing Ar before switching to a pyridine/Ar mixture (1 vol% pyridine, 40 mL·min⁻¹) for pyridine adsorption (0.5 h). The spectra were measured by averaging 20 scans at a resolution of 4 cm⁻¹ after purging the sample wafers with flowing Ar (40 mL·min⁻¹) at 150 and 200 °C for 1 h. Relative population of Lewis and Brønsted acidic sites on the catalyst surfaces was calculated using the integrated area of peaks at 1450 cm⁻¹ (for coordinated pyridine on Lewis acidic sites) and 1545 cm⁻¹ (for protonated pyridine on Brønsted acidic sites), assuming that the integrated molar extinction coefficients were 2.22 and 1.67 cm·μmol⁻¹, respectively, for pyridine adsorbed on Lewis and Brønsted acidic sites, as measured by Emeris.⁴⁷

1.3 Catalytic activity measurement

The MPV reaction of CAL with 2POL was performed at 150 °C and a molar ratio 2POL/CAL = 33 in a 25 mL stainless-steel autoclave batch reactor. Unless otherwise specified, the autoclave was loaded with 10 mL 2POL (AR, Dongfang Chemical Reagent Company, Beijing), 0.5 mL CAL (AR, Sigma-Aldrich, CAL), and 200 mg catalyst. After purging with dry N₂ (1.0 MPa) for six times, the autoclave was heated to the reaction temperature (150 °C) under 1 MPa dry N₂. Initiation of the reaction was done by switching on the stirring (900 rpm) as soon as the reaction temperature was reached. The stirring speed (900 rpm) for the reaction

was determined in preliminary experiments using varying stirring speeds (500-1200 rpm), which would guarantee absence of diffusion limitation during the catalytic reaction measurements. Termination of the reaction was done by dropping the autoclave in a water-ice bath to quench the reaction. Before workup, 0.5 mL dimethylformamide (DMF) was added as an internal standard into the reaction mixture. The liquid mixture was analyzed, after separation from the solid catalyst by filtration, on an HP7890 gas chromatography (GC) equipped with a Shimadzu HiCap CBP20-S25-050 capillary column (0.32 mm × 25 m) and an flame ionization detector (FID). As only cinnamyl alcohol (COL) and 1-cinnamyl 2-propyl ether (CPE) were detected as the reaction products in the reactor, the CAL conversion and product selectivity data were obtained according the calculations:

$$\text{CAL conversion (\%)} = \frac{\text{moles of CAL before rxn} - \text{mole of CAL after rxn}}{\text{mole of CAL before rxn}} \times 100\%$$

$$\text{Product selectivity (mol\%)} = \frac{\text{moles of a defined product}}{\text{mole of CAL consumed}} \times 100\%$$

The carbon balance of the reaction was estimated to be 98–108%.

Selective poisoning experiments using hindered pyridine (2,6-dimethyl pyridine or lutidine) or pyridine were carried out by injection prior to the reaction of different amounts of lutidine (99%, J&K Scientific Co., Ltd) or pyridine (99%, J&K Scientific Co., Ltd) into the reactor loaded with the reactants.

2. Results and discussion

2.1 Physicochemical properties of A-T and SA-T samples

Table 1 shows the BET surface area (S_{BET}), pore volume (V_{p}) and average pore diameter (D_{p}) data for the A-T and SA-T samples. The BET surface area declined from 413 to 50 $\text{m}^2 \cdot \text{g}^{-1}$ on increasing the calcination temperature T from 400 to 1000 °C for the A-T samples, accompanied by shrinking pore volume (0.38 to 0.20 $\text{cm}^3 \cdot \text{g}^{-1}$), pore diameter enlargement (3.5 to 12.9 nm), as well as phase transformation from $\gamma\text{-Al}_2\text{O}_3$ to $\theta\text{-Al}_2\text{O}_3$ when the calcination temperature was higher than 850 °C.^{49,50} For the SA-T samples, the calcination temperature effects on the BET surface area (382–270 $\text{m}^2 \cdot \text{g}^{-1}$), pore volume (0.73–0.67 $\text{cm}^3 \cdot \text{g}^{-1}$) and diameter (5.8–7.7 nm) were less prominent. Moreover, all the calcined SA-T ($T = 400\text{--}800$ °C) samples remained amorphous, as shown in Fig. 1, except that residual ammonium salts

were detected by diffractions at $2\theta = 26, 37$ and 49° . Thus, the existence of SiO_2 in the SA samples apparently improved the resistance of the co-existing Al_2O_3 towards sintering and crystallization.⁵¹

Table 1. Physical properties and surface acidity of A–*T* and SA–*T* samples

Sample	Physical properties				Acidic properties			
	S_{BET}^a ($\text{m}^2\cdot\text{g}^{-1}$)	V_{P}^a ($\text{cm}^3\cdot\text{g}^{-1}$)	D_{P}^a (nm)	Crystal phase ^b	Total acidity ^c ($\mu\text{mol}\cdot\text{m}^{-2}$)	BAS ^d density ($\mu\text{mol}\cdot\text{m}^{-2}$)	LAS ^e density ($\mu\text{mol}\cdot\text{m}^{-2}$)	B/L ^f
A-450	413	0.38	3.5	γ	1.28	0	1.28	0
A-600	316	0.36	4.0	γ	1.36	0	1.36	0
A-700	196	0.36	5.4	γ	1.94	0	1.94	0
A-800	160	0.37	6.5	γ	2.13	0	2.13	0
A-850	112	0.33	7.1	γ	2.86	0	2.86	0
A-900	68	0.24	12.1	θ	2.35	0	2.35	0
A-1000	50	0.20	12.9	θ	3.20	0	3.20	0
SA-400	396	0.73	5.8	a ^h	0.96 ^g	0.17	0.79	0.21
SA-500	395	0.74	5.8	a	1.10	0.21	0.83	0.25
SA-600	402	0.75	5.9	a	1.04	0.27	0.77	0.35
SA-700	382	0.74	6.0	a	1.10	0.25	0.85	0.30
SA-800	270	0.67	7.7	a	1.56	0.28	1.29	0.21

^a BET surface area (S_{BET}), pore volume (V_{P}) and pore diameter (D_{P}) estimated using the well-known BJH model.⁴⁸ ^b Crystal phase determined by XRD. ^c Determined by NH_3 -TPD. ^d Brønsted acidic site (BAS) ^e Lewis acidic site (LAS). ^f Molar BAS-to-LAS ratio. ^g This number was obtained by subtraction of the residual NH_4^+ salts from the desorbed NH_3 in the NH_3 -TPD measurement. ^h Amorphous.

NH_3 -TPD and IR spectroscopy of adsorbed pyridine were conducted to measure the surface acidity of the A–*T* and SA–*T* samples. The data for the A–*T* samples were reported in ref 41, which are also listed in Table 1 for comparison with those measured here in this study for the SA–*T* samples. No surface Brønsted acidic sites (BAS) was detected for the A–*T* samples, and the Lewis acidic site density for these samples increased with the calcination temperature.

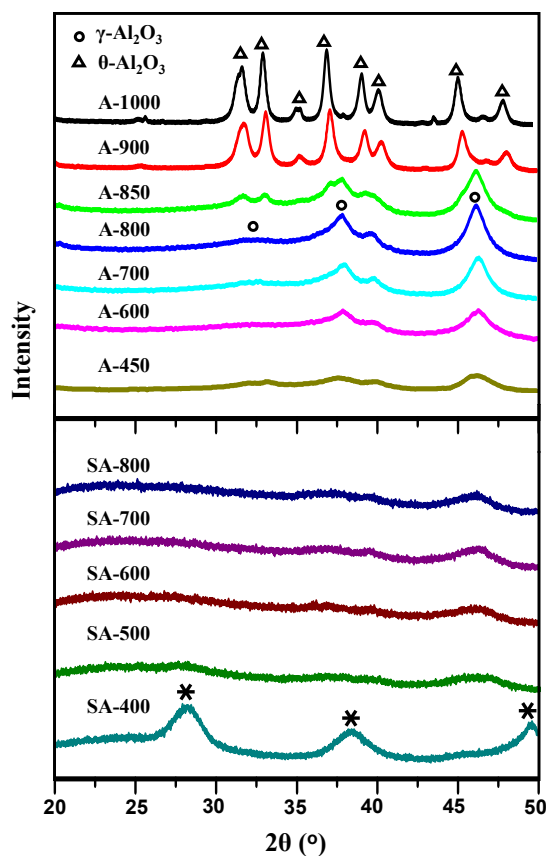


Figure 1. XRD profiles of A-*T* and SA-*T* samples. The asterisks (*) mark the diffractions from residual ammonium nitrate.

The NH₃-TPD profiles for the SA-*T* samples except SA-400 (Fig. 2A) feature a broad peak with maxima at ca. 200 °C. Increasing the calcination temperature *T* generally lowered the intensity of the peak but had little effect on the shape of the NH₃-TPD peak. The SA-400 sample seems unique, which gave a shoulder peak on the high temperature side (ca. 470 °C). This high temperature shoulder peak can be arisen from decomposition of residual ammonium ions (NH₄⁺) in the sample. This assignment was further corroborated in Fig. 2B, which shows a thermogravimetry–MS analysis (TGA/MS) of a fresh SA-400 sample and clearly detected a weight loss in the temperature range of 400–800 °C; the MS signals reveal evolutions of NH₃ and H₂O. The presence of NH₄⁺-involving entities in the fresh SA-400 sample were also detected as ammonium salts by XRD (Fig.1). Therefore, this SA-400 sample contained residual NH₄⁺ ions before NH₃ adsorption, which was deduced from the NH₃-TPD acidity for measuring the surface acidity of SA-400.

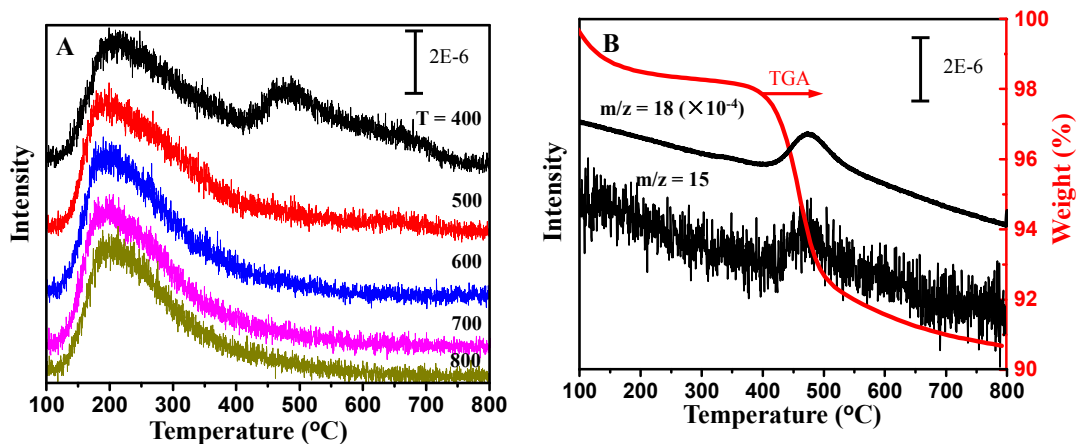
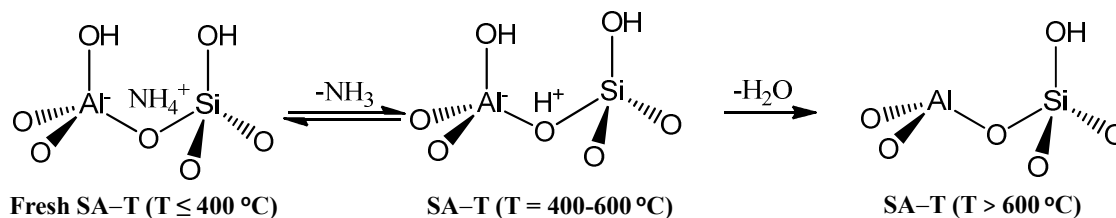


Figure 2. (A) NH_3 -TPD profiles of SA- T samples, and (B) TGA/MS curves of SA-400.

Figure 3 shows the FTIR spectra of chemisorbed pyridine on the SA- T samples. The absorption band centered at 1450 cm^{-1} features coordinately adsorbed pyridine on surface Lewis acidic sites (LAS) or coordinately unsaturated surface Al^{3+} sites on the surface of the SA samples.⁴¹ The absorption band centered at 1545 cm^{-1} is characteristic of surface pyridinium ion or protonated pyridine due to pyridine adsorption on BAS. Both of these absorption bands (1450 cm^{-1} and 1545 cm^{-1}) were significantly weakened with increasing the purging temperature from 150 to 200 °C (Fig. 3 A and B). Figure 3C shows the corresponding BAS-to-LAS ratios (B/L) according to the purging temperature for every SA- T sample. Regardless of purging temperature (150 or 200 °C), the sample calcined at 600 °C (i.e., SA-600) showed the maximum B/L ratios; the increase with T of B/L at the lower temperature side ($T \leq 600\text{ °C}$) would be accounted for by proton (BAS) generation as a result of NH_4^+ decomposition due to the use of a higher temperature for the sample calcination, while the decrease with T of B/L at $T \geq 600\text{ °C}$ can be explained by generation of LAS due to surface dehydroxylation, as depicted in Scheme 2.



Scheme 2. Evolution of Brønsted and Lewis acidic sites on SiO_2 - Al_2O_3 samples.

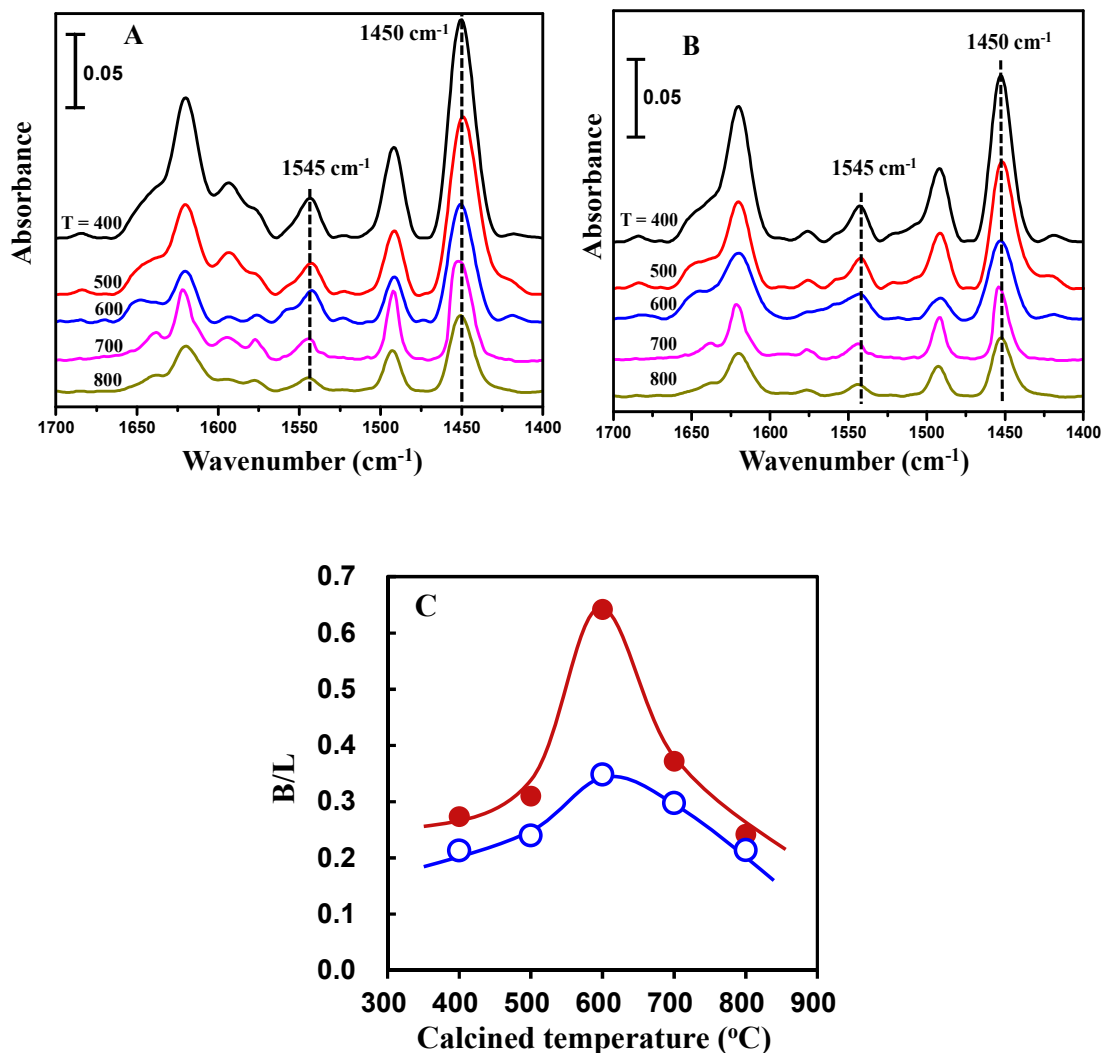


Figure 3. FTIR spectra of adsorbed pyridine on SA-T samples after purging in flowing Ar at (A) 150 °C and (B) 200 °C, respectively. (C) Effect of calcination temperature on the molar BAS-to-LAS (B/L) ratio after purging at 150 °C (○) and 200 °C (●).

The density of BAS and LAS on the surface of each SA-T sample can be therefore determined according to the total surface acidity obtained in the NH₃-TPD measurements and the B/L ratio obtained in the FTIR measurements of adsorbed pyridine. It should be noted that we employed the B/L ratios obtained from the FTIR spectra collected after purging at 150 °C, as the temperature of the transfer hydrogenation reaction of CAL and 2POL (presented in the next section) was set at 150 °C. The obtained results are listed in Table 1. It is seen that Lewis acidity (0.77–1.29 μmol·m⁻²) was always higher than Brønsted acidity (0.17–0.28 μmol·m⁻²) on the SA catalysts, agreeing with earlier documentaion.⁵²⁻⁵⁴

2.2 Catalytic performance of A-*T* and SA-*T* for Transfer hydrogenation of CAL and 2POL: insight into the nature of surface active sites

The MPV reaction or transfer hydrogenation of CAL and 2POL was conducted at 150 °C under mass-transfer free conditions using 200 mg catalyst, unless otherwise specified. Table 2 presents the catalytic performance data of every A-*T* and SA-*T* sample, together with the surface Lewis acidity data for the catalysts. The reaction was also conducted using a smaller amount of catalyst (20 mg) to limit the CAL conversion to less than ca. 6% for reliable measurement of the specific activity of the catalysts, and the data in the parentheses of Table 2 give the CAL conversion and COL selectivity in these reaction tests. Note that COL was always the only product over the different A-*T* catalysts, except a co-production of acetone (not shown) from the H-donor (2POL). However, CPE, a product of cascade cross-etherification between COL and 2POL,^{49,50} was always detected together with COL over the SA-*T* catalysts, and the selectivity for CPE clearly increased with the CAL conversion.

The areal activity data in Table 2 are obtained by normalizing the catalytic reaction rates measured at CAL conversion levels of lower than ca. 6% to the catalyst surface areas. The areal activity for A-*T* samples of $T = 450\text{--}850$ °C increased with increasing T from $0.61\ \mu\text{mol}\cdot\text{min}^{-1}\cdot\text{m}^{-2}$ for A-450 to $0.65\ \mu\text{mol}\cdot\text{m}^{-2}\cdot\text{min}^{-1}$ for A-600, and then to $1.55\ \mu\text{mol}\cdot\text{m}^{-2}\cdot\text{min}^{-1}$ for A-850. Despite of their high surface Lewis acidity ($2.35\text{--}3.2\ \mu\text{mol}\cdot\text{m}^{-2}$), the areal activity for the two $\theta\text{-Al}_2\text{O}_3$ -based samples (i.e., A-900 and A-1000) were much lower ($0.24\text{--}0.35\ \mu\text{mol}\cdot\text{m}^{-2}\cdot\text{min}^{-1}$) than that for the other A-*T*. The lower catalytic activity of these $\theta\text{-Al}_2\text{O}_3$ -based samples would be related to the fact that the Lewis acidity on the surface of $\theta\text{-Al}_2\text{O}_3$ was significantly weaker than that of $\gamma\text{-Al}_2\text{O}_3$,⁴¹ as stronger Lewis acidic sites would be more efficient in catalyzing the MPV reaction.^{55,56}

Compared with A-*T*, the SA-*T* samples showed lower areal activity and lower selectivity for COL in the MPV reaction of this study. The Lewis acid site density increased with increasing the calcination temperature T of the SA-*T* samples, from $0.79\ \mu\text{mol}\cdot\text{m}^{-2}$ for $T = 400$ °C to $1.29\ \mu\text{mol}\cdot\text{m}^{-2}$ for $T = 800$ °C. Unlike in the case of A-*T* catalysts, the areal activity of these SA-*T* samples showed an insignificant dependence on T and LAS density.

However, the selectivity for COL over these SA-*T* samples declined to less than 35 mol% and the major product became CPE (> 65 mol%) when the CAL conversion was made higher than 20%. BAS on the surface of the SA-*T* samples should be responsible for the formation of CPE as it was at all not observed over all of the A-*T* catalysts having only LAS.

Table 2. Lewis acid site density and catalytic performance at 150 °C of A-*T* and SA-*T* catalysts

Catalyst	LAS density ($\mu\text{mol}\cdot\text{m}^{-2}$)	CAL conv. ^a (%)	COL sel. ^a (mol%)	Areal activity ^b ($\mu\text{mol}\cdot\text{m}^{-2}\cdot\text{min}^{-1}$)	TOF ^b (min^{-1})
A-450	1.28	41.7 (8.3)	>99 (>99)	0.61	0.52
A-600	1.36	40.7 ^c (6.2)	>99 (>99)	0.65	0.48
A-700	1.94	47.8 (6.1)	>99 (>99)	1.04	0.53
A-800	2.13	38.5 (5.2)	>99 (>99)	1.08	0.51
A-850	2.86	44.1 (4.8)	>99 (>99)	1.43	0.50
A-900	2.35	4.8	>99 (>99)	0.24	0.10
A-1000	3.20	5.3	>99 (>99)	0.35	0.11
SA-400	0.79	19.2 ^d (3.0)	35.1 ^e (91.6) ^e	0.25	0.31
SA-500	0.83	21.6 ^d (2.9)	32.7 ^e (92.3) ^e	0.24	0.30
SA-600	0.77	23.1 (3.1)	28.4 ^e (90.6) ^e	0.26	0.33
SA-700	0.85	21.1 (3.0)	31.5 ^e (92.1) ^e	0.26	0.31
SA-800	1.29	23.1 (3.5)	33.2 ^e (93.2) ^e	0.43	0.34

Rxn conditions: 0.5 mL CAL, 10 mL 2POL, 1.0 MPa N₂, 900 rpm, 1 h. ^a Number outside the parenthesis shows the conversion over 200 mg catalyst while those in the parenthesis over 20 mg catalyst; ^b Obtained at CAL conversion of no higher than ca. 8%; ^c 35 min; ^d 4 h; ^e The balance (i.e., 100%– COL selectivity) gives the selectivity for CPE.

In order to further understand the nature of the active sites on the catalyst surface for the MPV reaction, hindered pyridine (2,6-dimethyl pyridine or lutidine) and pyridine were added, respectively, to the reaction mixture in varying amounts for investigating possible effects of their poisoning to the acidic sites on the catalyst surface. The hindered pyridine has known as a specific poison to BAS while pyridine a non-specific poison to both BAS and LAS.^{42,57,58} Using SA-600 as a representative SA catalyst, Fig. 4 shows effects of lutidine and pyridine addition on CAL conversion and product selectivity of the MPV reaction over

SiO₂-Al₂O₃ catalysts. The addition of even small amounts of lutidine (e.g., molar lutidine/BAS < 0.1) produced a remarkable effect on the product selectivity: the selectivity for COL was significantly enhanced at the expense of CPE (Fig. 4A). The selectivity for COL was kept on increasing with the amount of added lutidine until lutidine/BAS ≥ 1, when the formation of CPE (from the cascade cross-etherification reaction) was completely inhibited and COL became the only product from CAL. However, the addition of lutidine had no effect on the reactivity of CAL, whose conversion level was kept constant regardless of the amount of added lutidine (Fig. 4A). These results clearly confirm that BASs have nothing to do with the COL-producing MPV reaction but are responsible for catalyzing the cascade cross-etherification reaction.

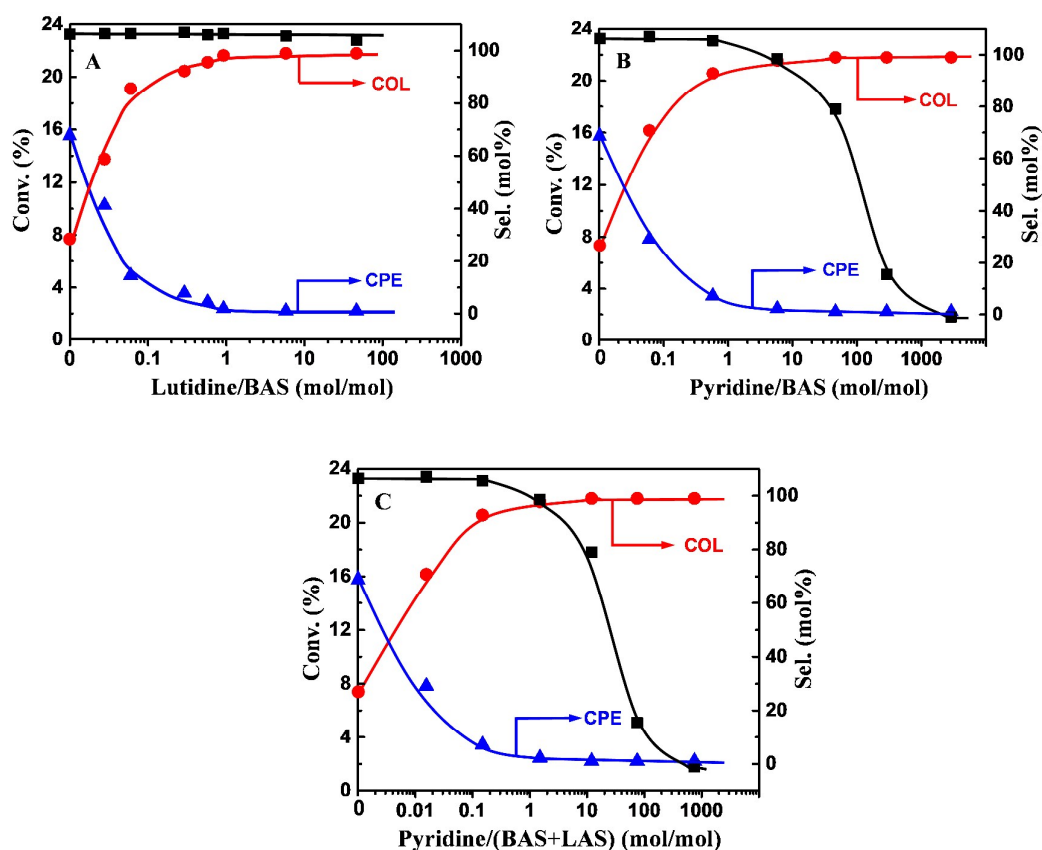
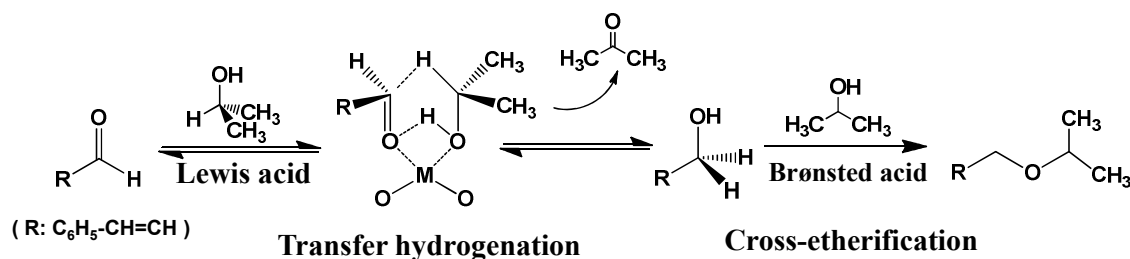


Figure 4. Poisoning effects of lutidine (A) and pyridine (B and C) during the MPV reaction of CAL and 2POL on CAL conversion (■), and selectivity for COL (●) and CPE (▲) over SA-600. Other conditions: 200 mg catalyst, 0.5 mL CAL, 10 mL 2POL, 1.0 MPa N₂, 900 rpm, 1 h.

Similar effects were observed when small amounts of pyridine [pyridine/BAS < ca. 0.5

or pyridine/(BAS + LAS) < ca. 0.1] were added; the selectivity for COL increased while that for CPE decreased, with the reactivity of CAL being little affected (Fig. 4 B and C). Both the reactivity of CAL and product selectivity became sensitively affected, however, when higher amounts of pyridine were added to reaction mixture. The sensitiveness of the product selectivity and relative insensitiveness of the CAL reactivity to the addition of small amounts of pyridine would indicate that the surface BAS is more sensitive than the LAS to the poisonous pyridine. Therefore, adsorption of pyridine on surface BAS was stronger than on LAS. These results further confirm that the LASs were responsible for catalyzing the COL-producing MPV reaction¹²⁻¹⁴ while the BASs for catalyzing the cascade cross-etherification,³⁸⁻⁴⁰ as highlighted in Scheme 3.



Scheme 3. Heterogeneous Lewis acid catalyzed MPV reaction of CAL with 2POL, followed by cascade cross-etherification via Brønsted acid catalysis.

The selective poisoning experiments were also conducted with the γ -Al₂O₃ catalysts. Table 3 shows the results over A-600. Regardless of the amounts of added lutidine, the reactivity of CAL and selectivity for COL were not at all affected by the added lutidine. This completely inertness of the MPV reaction to the addition of this BAS-specific poison well demonstrates that the surface of γ -Al₂O₃ does not have BAS⁵⁹ and thus excludes the possibility of BAS participation in catalyzing the MPV reaction. In contrast, the reactivity (conversion) of CAL was lowered significantly when the non-specific pyridine was added instead of lutidine, due pyridine poisoning of the catalytic LASs on the catalyst (γ -Al₂O₃) surface. The MPV reaction was also carried out under high-pressure CO₂ on the A-600 catalyst, attempting to gain an insight into a possible effect of CO₂ poisoning of the surface basic sites. As indicated by the data shown in the bottom of Table 4, the MPV reaction was also completely insensitive to the presence of even a large amount of CO₂ (2 MPa). This

insensitiveness to CO₂-poisoning suggests no participation of surface basic sites in catalyzing the MPV reaction.

Table 3. Poisoning effects of lutidine, pyridine and CO₂ on the MPV reaction at 150 °C over A-600

Poison	N _{poison} (mmol)	n _{poison} /n _{total acidity} (mol/mol)	CAL conv. (%)	COL sel. (%)
lutidine	0	0.0	40.7	>99
	4.3	50.2	40.2	>99
	8.0	93.0	40.5	>99
	43 ^a	502.3	38.5	>99
pyridine	0	0.0	40.7	>99
	0.2	2.3	35.1	>99
	1.0	11.6	33.4	>99
	2.0	23.3	32.8	>99
	8.0	93.0	24.7	>99
	62 ^b	726.7	8.1	>99
CO ₂	14.4 ^c	-	40.1	>99

Other conditions: 200 mg catalyst, 0.5 mL CAL, 10 mL 2POL, 1.0 MPa N₂, 900 rpm, 35 min. ^a 5 mL lutidine (hindered pyridine), 5 mL 2POL. ^b 5 mL pyridine, 5 mL 2POL. ^c 2 MPa CO₂.

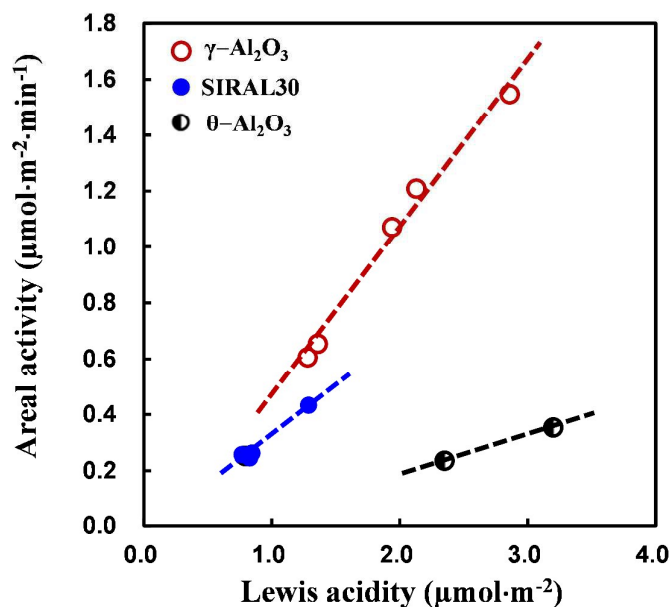


Figure 5. Correlation between the catalytic activity and surface Lewis acidity of the A-T and SA-T catalysts.

We therefore have reason to correlate the catalyst activity for the MPV reaction with the number of LAS on the catalyst surface. The correlation is presented in Fig. 5 by plotting the catalyst areal activity ($\mu\text{mol}\cdot\text{m}^{-2}\cdot\text{min}^{-1}$) against the LAS density at the catalyst (A–T and SA–T) surfaces. Again, the relationships between the areal activity and the LAS density (or surface Lewis acidity) for the serial $\gamma\text{-Al}_2\text{O}_3$ (A–T of $T \leq 850$ °C) and SA catalysts demonstrate that the catalyst surface Lewis acidity is responsible for the hydrogen-transfer catalysis.¹²⁻¹⁴ Note that the dependence slope for the A–T samples was significantly higher than for the SA–T ones, which would be related with the effect of Lewis acidity strength on the catalyst activity.^{55,56} Indeed, the average acidity strength of LASs on the surface of A–T was stronger than that on the surface of SA–T as the highest temperature of the NH_3 -TPD profiles extended to ca. 600 °C for A–T of $T \leq 850$ °C⁴¹ but no higher than 500 °C for SA–T (Fig. 2). The even much bigger activity difference between $\theta\text{-Al}_2\text{O}_3$ (A–T of $T \geq 900$ °C) and $\gamma\text{-Al}_2\text{O}_3$ (A–T of $T \leq 850$ °C) catalysts further confirms the effect of Lewis acidity strength on the catalysis by LAS. As we showed earlier,⁴¹ the surface Lewis acidity of $\gamma\text{-Al}_2\text{O}_3$, characterized by the highest temperature of the NH_3 -TPD profile, would be much stronger than that of $\theta\text{-Al}_2\text{O}_3$. The last column of Table 2 shows the catalytic turnover frequency (TOF) per LAS, which was obtained by normalizing the catalytic reaction rates measured at CAL conversion of lower than ca. 6% to the density of LAS on the catalyst surface. Again, the respectively similar TOF numbers for $\gamma\text{-Al}_2\text{O}_3$ (A–T of $T \leq 850$ °C, 0.5 min^{-1}), $\text{SiO}_2\text{-Al}_2\text{O}_3$ (SA–T, 0.3 min^{-1}) and $\theta\text{-Al}_2\text{O}_3$ (A–T of $T \geq 900$ °C, 0.1 min^{-1}) catalysts are consistent in supporting the conclusion that the specific activity by TOF of CAL consumption is determined mainly by the Lewis acidity strength.

3. Conclusions

This work compares the catalytic performance of serial Al_2O_3 and $\text{SiO}_2\text{-Al}_2\text{O}_3$ catalysts in the MPV reaction of CAL with 2POL and correlates the performance with the catalyst surface acidity and nature (type) of the acidic sites. The catalytically active sites are identified as the surface LASs that are insensitive to the poisoning of hindered pyridine (lutidine). The surface BASs appear to be among the spectator sites during the MPV reaction but they serve as the active sites for catalyzing the cascade cross-etherification reaction

between COL and 2POL, reducing the selectivity for COL. Also, LAS of stronger acidity is found to show higher activity for the MPV reaction. A possible involvement of surface basic sites during the reaction is reasonably excluded by comparing the reactivity of CAL under the presence and absence of higher pressure CO₂.

Acknowledgements

This work was supported by the National Natural Science Foundation of China (grants: 21533004 and U1463208) and the National Basic Research Program of China (grant: 2013CB933103).

References

1. C. F. Degrauw, J. A. Peters, H. Vanbekkum and J. Huskens, *Synthesis (Stuttgart)*, 1994, **10**, 1007-1017.
2. J. R. Ruiz and C. J. Sanchidrian, *Curr. Org. Chem.*, 2007, **11**, 1113-1125.
3. G. K. Chuah, S. Jaenicke, Y. Z. Zhu and S. H. Liu, *Curr. Org. Chem.*, 2006, **10**, 1639-1654.
4. J. S. Cha, *Org. Process Res. Dev.*, 2006, **10**, 1032-1053.
5. Y. C. Hong, K. Q. Sun, G. R. Zhang, R. Y. Zhong and B. Q. Xu, *Chem. Commun.*, 2011, **47**, 1300-1302.
6. K. Q. Sun, Y. C. Hong, G. R. Zhang and B. Q. Xu, *ACS Catal.*, 2011, **1**, 1336-1346.
7. P. Claus, *Top. Catal.*, 1998, **5**, 51-62.
8. L. M. Jackman and J. A. Mills, *Nature*, 1949, **164**, 789-790.
9. E. D. Williams, K. A. Krieger and A. R. Day, *J. Am. Chem. Soc.*, 1953, **75**, 2404-2407.
10. V. A. Ivanov, J. Bachelier, F. Audry and J. C. Lavalley, *J. Mol. Catal.*, 1994, **91**, 45-59.
11. J. L. Song, B. W. Zhou, H. C. Zhou, L. Q. Wu, Q. L. Meng, Z. M. Liu and B. X. Han, *Angew. Chem., Int. Ed.*, 2015, **54**, 9399-9403.
12. V. L. Sushkevich, I. I. Ivanova, S. Tolborg and E. Taarning, *J. Catal.*, 2014, **316**, 121-129.
13. H. Y. Luo, D. F. Consoli, W. R. Gunther and Y. R. Leshkov, *J. Catal.*, 2014, **320**, 198-207.

14. P. P. Samuel, S. Shylesh and A. P. Singh, *J. Mol. Catal. A: Chem.*, 2007, **266**, 11-20.
15. M. Glinski, A. Czajka and U. Ulkowska, *React. Kinet., Mech. Catal.*, 2015, **114**, 279-294.
16. M. Glinski, *Appl. Catal., A*, 2008, **349**, 133-139.
17. M. Glinski and U. Ulkowska, *Pol. J. Chem.*, 2008, **82**, 1117-1119.
18. F. Wang, N. Ta and W. Shen, *Appl. Catal., A*, 2014, **475**, 76-81.
19. J. K. Bartley, C. Xu, R. Lloyd, D. I. Enache, D. W. Knight and G. J. Hutchings, *Appl. Catal., B*, 2012, **128**, 31-38.
20. J. J. Ramos, V. K. Diez, C. A. Ferretti, P. A. Torresi, C. R. Apesteguia and J. I. Di Cosimo, *Catal. Today*, 2011, **172**, 41-47.
21. V. K. Diez, C. A. Ferretti, P. A. Torresi, C. R. Apesteguia and J. I. Di Cosimo, *Catal. Today*, 2011, **173**, 21-27.
22. M. Mora, M. I. Lopez, C. J. Sanchidrian and J. R. Ruiz, *Catal. Lett.*, 2010, **136**, 192-198.
23. Z. Boukha, L. Fitian, M. L. Haro, M. Mora, J. R. Ruiz, C. J. Sanchidrian, G. Blanco, J. J. Calvino, G. A. Cifredo, S. Trasobares and S. Bernal, *J. Catal.*, 2010, **272**, 121-130.
24. M. Glinski and U. Ulkowska, *React. Kinet. Catal. Lett.*, 2008, **95**, 107-112.
25. F. O. Figueras, *Top. Catal.*, 2004, **29**, 189-196.
26. J. I. Di Cosimo, A. Acosta and C. R. Apesteguia, *J. Mol. Catal. A: Chem.*, 2004, **222**, 87-96.
27. T. Komanoya, K. Nakajima, M. Kitano and M. Hara, *J. Phys. Chem. C*, 2015, **119**, 26540-26546.
28. J. Wang, S. Jaenicke and G. K. Chuah, *RSC Adv.*, 2014, **4**, 13481-13489.
29. C. J. Sanchidrian and J. R. Ruiz, *Appl. Catal., A*, 2014, **469**, 367-372.
30. J. M. Hidalgo, C. J. Sanchidrian and J. R. Ruiz, *Appl. Catal., A*, 2014, **470**, 311-317.
31. V. Borzatta, E. Capparella, R. Chiappino, D. Impala, E. Poluzzi and A. Vaccari, *Catal. Today*, 2009, **140**, 112-116.
32. S. Axpuac, M. A. Aramendia, J. H. Carrillo, A. Marinas, J. M. Marinas, V. M. Jimenez, F. J. Urbano and V. Borau, *Catal. Today*, 2012, **187**, 183-190.
33. F. J. Urbano, M. A. Aramendia, A. Marinas and J. M. Marinas, *J. Catal.*, 2009, **268**,

79-88.

34. Y. Z. Zhu, S. H. Liu, S. Jaenicke and G. K. Chuah, *Catal. Today*, 2004, **97**, 249-255.
35. J. F. Minambres, M. A. Aramendia, A. Marinas, J. M. Marinas and F. J. Urbano, *J. Mol. Catal. A: Chem.*, 2011, **338**, 121-129.
36. M. Boronat, A. Corma and M. Renz, *J. Phys. Chem. B*, 2006, **110**, 21168-21174.
37. R. Cohen, C. R. Graves, S. B. T. Nguyen, J. M. L. Martin and M. A. Ratner, *J. Am. Chem. Soc.*, 2004, **126**, 14796-14803.
38. J. Iglesias, J. A. Melero, G. Morales, J. Moreno, Y. Segura, M. Paniagua, A. Cambra and B. Hernandez, *Catal.* 2015, **5**, 1911-1927.
39. S. H. Liu, S. Jaenicke and G. K. Chuah, *J. Catal.*, 2002, **206**, 321-330.
40. Y. Zhu, G. K. Chuah and S. Jaenicke, *J. Catal.*, 2006, **241**, 25-33.
41. Z. Hu, W. Z. Li, K. Q. Sun and B. Q. Xu, *Catal. Sci. Technol.*, 2013, **3**, 2062-2071.
42. Y. R. Xing, B. Yan, Z. F. Yuan and K. Q. Sun, *RSC Adv.*, 2016, **6**, 59081-59090.
43. L. Z. Tao, B. Yan, Y. Liang and B. Q. Xu, *Green Chem.*, 2013, **15**, 696-705.
44. B. Yan, L. Z. Tao, Y. Liang and B. Q. Xu, *ChemSuschem*, 2014, **7**, 1568-1578.
45. B. Yan, A. Mahmood, Y. Liang and B. Q. Xu, *Catal. Today*, 2016, **269**, 65-73.
46. B. Yan, L. Z. Tao, A. Mahmood, Y. Liang and B. Q. Xu, *ACS Catal.*, 2017, **7**, 538-550.
47. C. A. Emeis, *J. Catal.*, 1993, **141**, 347-354.
48. E. P. Barrett, L. G. Joyner and P. P. Halenda, *J. Am. Chem. Soc.*, 1951, **73**, 373-380.
49. C. Pecharroman, I. Sobrados, J. E. Iglesias, T. G. Carreno and J. Sanz, *J. Phys. Chem. B*, 1999, **103**, 6160-6170.
50. M. Trueba and S. P. Trasatti, *Eur. J. Inorg. Chem.*, 2005, 3393-3403.
51. S. F. Yin and B. Q. Xu, *ChemPhysChem*, 2003, **4**, 277-279.
52. K. Tanabe, *Stud. Surf. Sci. Catal.*, 1989, **51**, 117-119.
53. S. Nassreddine, S. Casu, J. L. Zotin, C. Geantet and L. Piccolo, *Catal. Sci. Technol.*, 2011, **1**, 408-412.
54. M. Stekrova, H. Minarikova, E. Vyskocilova, J. Kolena and L. Cervený, *J. Porous Mater.*, 2014, **21**, 757-767.
55. J. Wang, K. Okumura, S. Jaenicke and G. K. Chuah, *Appl. Catal., A*, 2015, **493**,

112-120.

56. J. Wang, S. Jaenicke and G. K. Chuah, *RSC Adv.*, 2014, **4**, 13481-13489.

57. P. A. Jacobs and C. F. Heylen, *J. Catal.*, 1974, **34**, 267-274.

58. J. G. Santiesteban, J. C. Vartuli, S. Han, R. D. Bastian and C. D. Chang, *J. Catal.*, 1997, **168**, 431-441.

59. Q. L. Dai, B. Yan, Y. Liang, B. Q. Xu et al., *Catal. Today*, 2017, 295, 110-118.

TOC graphic:

Surface Brønsted acidic and basic sites are neither involved in the catalytic transfer hydrogenation reaction of Cinnamaldehyde with 2-Propanol.

